Available online at www.sciencedirect.com

ScienceDirect

Energy Procedia 148 (2018) 720–727

Energy Procedia

www.elsevier.com/locate/procedia

73rd Conference of the Italian Thermal Machines Engineering Association (ATI 2018), 12–14 September 2018, Pisa, Italy

Heat exchanger design and optimization by using genetic algorithm for externally fired micro-turbine

E. Fanelli[a]*, N. Lovaglio[b], G. Cornacchia[a], G. Braccio[a] and V. Magi[b]

[a] *ENEA - Italian National Agency for New Technologies, Energy and Sustainable Economic Development - S.S. Jonica 106 km 419+500, 75026 Rotondella, MT, Italy*

[b] *University of Basilicata - School of Engineering - Viale dell'Ateneo Lucano, 10 - 85100 Potenza, Italy*

Abstract

In this study, a new configuration where syngas produced by downdraft gasifier is feed directly in an externally fired air turbine is discussed. Attention was posed towards the critical component of this configuration: the heat exchanger. To achieve acceptable electrical efficiencies, high temperature of the air at the inlet turbine section was imposed. A code for heat exchanger design was built by using Matlab®, while the geometrical optimization was performed by using modeFRONTIER® by imposing a multi-objective function to maximize the overall heat transfer coefficient and minimize both costs and pressure drops across the equipment.

Keywords: *Biomass Gasification; Downdraft Gasifier; Externally Fired Air Turbine; Heat Exchanger; Multi-objective Optimization*

1. Introduction

The continuous growth of the worldwide energy demand together the irreversible depletion of traditional fossil fuels, implies to search new ways for energy production and/or conversion.

* Corresponding author. Tel.: +39 835 974445; fax: +39 835 974210.
E-mail address: emanuele.fanelli@enea.it

10.1016/j.egypro.2018.08.162

Nomenclature

A	area [m^2]	$k_{L,bc}$	buffle spacing parameter
A_m	effective mean wall heat transfer area [m^2]	k_w	wall resistance [W/m K]
A_o	total heat transfer area [m^2]	$LMTD$	log mean temperature difference
c_p	heat capacity [J/kg K]	$L_{t,i}$	tube length [m]
C_t	heat exchanger purchase cost [k€]	L_{bc}	central buffle spacing [m]
d	tube diameter [m]	L_{tp}	tube pitch [m]
D_s	shell inside diameter [m]	m	mass flow rate [kg/s]
F	$LMTD$ correction factor	N_p	tubeside number of passage
G	mass velocity [kg/m^2 s]	N_t	tube number
h	heat transfer coefficient [W/m^2 K]	Pr	Prandtl number
h_i	heat transfer coefficient for pure crossflow [W/m^2 K]	q	thermal power [W]
h_s	shellside heat transfer coefficient [W/m^2 K]	r	tube radii [m]
j_i	Colburn factor	Re	Reynolds number
J_c	correction factor for buffle cut and spacing	R_f	fouling resistance [m^2 K/W]
J_b	correction factor for the bundle bypass flow	T	temperature [K]
J_l	correction factor for baffle leakage effects	t_w	tube wall thickness [mm]
J_r	correction factor for adverse temperature gradient	U	global heat transfer coefficient [W/m^2 K]
J_s	correction factor for variable baffle spacing in the inlet and outlet sections	v_t	tubeside flow velocity [m/s]
k	thermal conductivity [W/m K]	ϕ	viscosity correction factor
k_{layout}	geometrical parameter for tube arrangement	ΔP	pressure drop [Pa]
$k_{L,tp}$	tube pitch parameter		

Subscript

air	air	i	inlet, inside
c	cold	o	outlet, outside
ex	exhaust gases	s	shellside
h	hot	t	tubeside

Because of their renewable nature and widespread availability, the use of alternative fuels such as biomass is one of the most promising solution. Today different technologies are available, but among these only those for which energy is produced locally at small scale (below 100 kW$_e$) by residual biomass have gained attention in recent years. In energy production two major aspects are to be taken into account: reduce the costs of production and minimize the effect on environment [1]. To meet these conditions, technologies used must guarantee simpleness in construction, reliable operation, suitability for different kinds of biomass feedstock, acceptable net efficiency and low pollutant emissions [2]. Following the thermochemical conversion pathway, gasification seems to cross better these requirements. This is because gasification implies, for a given biomass power input, lowest dimensions in plant development (i.e. size of the reactor, piping and utilities) and highest efficiency in energy conversion. For small-scale distributed power applications (i.e. in the range 10 kW – 250 kW), downdraft gasifiers are considered the most suitable technology because of their intrinsic simple fabrication and operation. The gas leaving the gasifier is substantially a mixture of combustible (CO, H_2 and CH_4) and non-combustible (CO_2, N_2, H_2O) molecules in a fraction that is function of the different operational parameters of the process. Other compound (contaminants) like tars are always present in the producer gas in a measure that is function of the technology used (in the order of 1 g/Nm^3 is downdraft is used). The syngas leaving the reactor is then purified and it is now ready for applications. Due to its very low heating value, syngas from downdraft gasifier is mainly applied as fuel in internal combustion engines for power production [3] or in gas burner for direct combustion for heat production. Despite the undisputed advantages of downdraft gasifiers, drawbacks such as grate blocking, bridging and channeling are typically found when low bulk density feedstocks are used. Furthermore, downdraft gasifiers are suitable for low moisture content feedstocks, typically below 30% wt. Higher moisture content affects the syngas quality in term of its heating value and then the gasification cold efficiency. Also tar reduction is negatively affected. This is because higher quantities of reaction heat must be devoted to biomass drying reducing consequently the reaction temperature. To remedy this, a series of improvements have been worldwide proposed by researchers at reactor design level. A comprehensive review is reported by [4] . For ICE (Internal Combustion Engine) applications the primary limiting factor in the use of gasification technology and that greatly affect its commercial dissemination, is the syngas tar content. ICE imposes stringent limits in term of syngas contaminants: in addition to the usual ones (sulfur and chloride), below 10 - 20 mg/Nm^3 for both tars and particulate to guarantee long time operation. This requires auxiliary plant equipment such as scrubbers (if wet methods are used) alongside the traditional ones (cyclones, impact filters and dry filter for dust and moisture abatement). Even though these solutions partially allow to meet the stringent limits imposed by ICE, expensive waste disposal procedures are added in the economy of the plant. Bio–oil can be efficiently reused in the system as energy additional source, but generally the excess in mass flow rate at the purge line of the scrubber respect to that where it is used as fuel for power supply, it means a bio-oil accumulation that must be consumed or disposed in other ways. In addition, downdraft to ICE applications imposes continuous adjustment in the engine power rating because of the variation of syngas quality (mainly LHV but also hydrogen to carbon monoxide ratio) as response at any modification of the input operational parameters (such as feedstock size and quality, [5]). Furthermore, the net electrical efficiency by different operational experiences hardly exceeds 18 - 20 % as reported by [6] . Surely downdraft gasifier coupled to ICE for small plant and distributed power generation is a good choice when residual biomass is available, but the above still unresolved questions, impose an accurate evaluation of the benefits achievable by this practice. As response to this and to partially overcome the above presented issues, in this study a new configuration is proposed. Syngas by a downdraft gasifier is directly burned at the reactor exit section to heat production. Heat is then used in an external heat exchanger to drive an externally air heated micro-turbine (MT). This solution allows to mitigate the impact of the gas cleaning section by reducing investments in equipment and operational costs for wastes disposal (tars, condensates and washing liquids). Furthermore, power production is decoupled by gas quality allowing the use of different material feedstock (compatible with the reactor design) without the need of continuous regulation at the power section. Also, the availability of the power engine is improved by reducing the operative maintenance needs by ICE (oil and filters substitution, piston rings, valves, spark plug, etc.) after few hours of operation (1000 – 1500 hr). Again, the combustion of syngas instead of biomass in a traditional furnace, implies a reduction in size at the reactor section and in turn in capex and in plant layout development. Drawbacks of this configuration are related at the need of an external high temperature heat exchanger (very expensive) and a more sophisticate control system. Again, the net electrical efficiency, for small scale applications, is in the order of 18 – 19% for regenerative heat exchanger layout. This work deals about the geometrical optimization of the critical component of the investigated plant configuration: the heat exchanger (the over-heater S1 as shown in Figure 1). With the aim to improve the overall plant efficiency, high temperatures (greater than 700°C) are required at the inlet turbine section. This means that the use of specific alloys for the heat exchanger fabrication and high capital investments are involved. Figure 1 shows a sketch of the plant configuration here considered for the evaluations. Syngas by downdraft gasifier is directly burned in a post-combustor and hot flue gases are used to drive an externally heated air turbine. Hot air by the turbine discharge section feeds the post-combustor to provide the primary combustion air. Hot air is also used as gasifying medium in the gasifier. A fraction of the flue combustion gases is recycled in the post-combustor to control the maximum gas temperature. In the regenerative layout here considered, the hot air from turbine feeds the regenerative section of the heat exchanger to preheat air from the compressor.

2. Mathematical model

A code for heat exchanger design was built by using Matlab®, while the geometrical optimization was performed by using a multi objective genetic algorithm (MOGA II) implemented in modeFRONTIER®. In order to maximize the overall heat transfer coefficient and minimize both costs and pressure drops across the equipment, a constrained multi-objective function was built and implemented in the simulative ambient. In the follows, models for each section are briefly discussed.

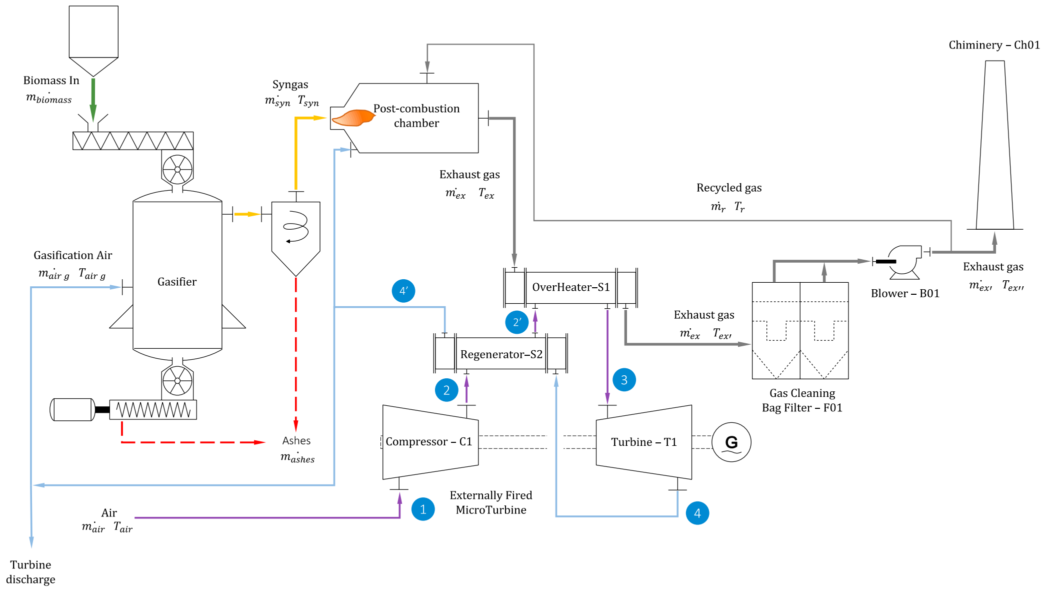

Figure 1. Plant regenerative layout

2.1. Heat exchanger model

Shell and tube type heat exchanger was selected for the purpose. Thought other type can be theoretically applied such as plate heat exchangers (higher global heat transfer coefficient and compactness), very high temperatures of flue gases (above 800°C, i.e. fabrication material issues) and fouling related issues (particulates such as incombustible char and condensable such as tars in the flue gas) drive the choice towards a more robust design. TEMA standards [7], applicable to unfired shell and tube with inside diameter up to 60 in. (i.e. 1524 mm), was used as reference. The detailed design method of Bell-Delaware [8] was instead implemented in Matlab® in order to perform calculations. The heat load was calculated by the general equation:

$$q = m_h c_{p,h}(T_{h,i} - T_{h,o}) = m_c c_{p,c}(T_{c,i} - T_{c,o})\ [W] \tag{1}$$

The greatest uncertainty in heat exchanger design is related at the estimation of the overall heat transfer coefficient here evaluated as:

$$U = \frac{1}{[(1/h_s) + R_{fo} + (t_w/k_w)(A_o/A_m) + (R_{fi} + 1/h_t)(A_o/A_i)]}\ [W/m^2\ K] \tag{2}$$

where $A_m = \pi L(r_o - r_i)$ is the effective mean wall heat transfer area that is approximated by the arithmetic mean area referred to the outside and inside tube radii r_i and r_o respectively. Fouling resistance factors R_{fo} and R_{fi} were instead derived from TEMA Table RGP-T-2.4. Once the total thermal power q, the global heat transfer coefficient U and the log mean temperature difference $LMTD$ are known, the global heat transfer area A_o can be evaluated.

Geometrical and auxiliary mathematical expressions involved in the Bell-Delawere method as well as those for the pressure drop evaluation, are here omitted. For exhaustive details, you can refer to the technical literature in the field [8], [9]. Only expressions used for the heat transfer coefficients are briefly presented in the follow. In the Bell-Delawere method, the shellside heat transfer coefficient h_i for the ideal crossflow is modified by considering different correction factors to approach the real flow pattern through the equipment. In this way, the shellside heat transfer coefficient can be expressed as:

$$h_s = h_i \cdot J_c \cdot J_l \cdot J_b \cdot J_s \cdot J_r \tag{3}$$

where

$$h_i = j_i \frac{c_{p,s} G_s}{Pr_s^{2/3}} \phi_s^{\ 0.14} \text{ with } j_i = \begin{cases} 1.73 Re_s^{-0.694}, & 1 \le Re_s < 100 \\ 0.717 Re_s^{-0.574}, & 100 \le Re_s < 1000 \\ 0.236 Re_s^{-0.346}, & 1000 \le Re_s \end{cases} \tag{4}$$

The tubeside heat transfer coefficient is instead evaluated as function of the Reynolds number by means the follows correlations:

$$\frac{h_t d_i}{k_i} = \begin{cases} 1.86 \left(Re_t Pr_t \frac{d_i}{L} \right)^{0.5} Pr_t^{1/3} \phi_t^{\ 0.14}, & 2100 < Re_t \\ 0.116 \left(Re_t^{\ 2/3} - 125 \right) \left[1 + \left(\frac{d_i}{L} \right)^{2/3} \right] Pr_t^{1/3} \phi_t^{\ 0.14}, & 2100 \le Re_t < 10000 \\ 0.027 \cdot Re_t^{\ 0.8} Pr_t^{1/3} \phi_t^{\ 0.14}, & 10000 \le Re_t \end{cases} \tag{5}$$

The heat exchanger total cost C_t was evaluated by using the followings correlations:

$$C_t = F_p \cdot F_M \cdot F_L \cdot C_B \tag{6}$$

where:

$$F_p = 0.9803 + 0.018 \frac{p}{100} + 0.0017 \left(\frac{p}{100} \right)^2$$ is pressure factor with p fluid pressure (psia) .

$$F_M = a + \left(\frac{A_o}{100} \right)^b$$ is the materials of construction factor with A_o total heat transfer area (ft^2) and a=3.3, b=0.08 for Alloy 800HT .

F_L is the tube-length correction factor function of the total tube length .

$$C_B = e^{[11.0545 - 0.9228 \ln(A_o) + 0.09861 \ln(A_o)^2]}$$ is the base investment cost for shell and tube heat exchanger with fixed head. A_o is total heat transfer area (ft^2) . (7)

2.2. Micro turbine thermodynamic model

Simple thermodynamic model was developed to get evaluations of the main cycle performances. Matlab® was used to implement the mathematical code by using CoolProp® libraries to evaluate fluid properties at each plant sections. For the purpose, the total heat subtracted at the over-heater S1 from the hot exhaust gases (i.e. the thermal load at the heat exchanger here investigated as expressed by Eq. (1)), can be evaluated as:

$$\dot{Q}_{S1} = q = m_{ex} \cdot \left(h_{ex,i} - h_{ex,o} \right) = m_{air} \cdot \left(h_3 - h_{2,1} \right) \ \ [W] \tag{8}$$

2.3. Multi-Objective optimization model

Otherwise than single-objective problems, multi-objective ones do not produce one solution, but instead a set of solutions well known as Pareto solutions, trade-off surface or Pareto frontier. By definitions [10], Pareto solutions are considered optimal because there are no other designs that are superior in all objectives. As previously mentioned, modeFrontier® was here used to perform the optimization process by adopting a Multi-Objective Genetic Algorithm (MOGA II). It requires to be provided with a number of test runs (the initial population) called design of experiments (DOEs). The DOEs is a sample of designs generated from the design spaces that will form the basis of the analysis, before the scheduler (MOGA II) takes over. The genetic algorithm MOGA II uses the experience achieved from these first runs to generate proper samples. The initial population contains 100 individuals that were generated by the deterministic algorithm SOBOL which was here used to fill uniformly the studied domain. In the same manner, 100 generations were set so that the optimization algorithm attempts a total number of 10000 evaluations (equal to the number of points in the DOE table, i.e. the initial population, multiplied by the number of generations) to bring the Pareto frontier.

3. Results

As Figure 2-(a) shows, the modeFrontier® optimization model uses eight main operational constants (temperatures, pressures and mass flow rate of fluids as reported in Table 1) and six geometrical and flow variables (tubeside flow velocity, Reynolds number, number of passes and tube layout constants as reported in Table 2) to perform 10000 evaluations of the two main objective functions. Only one constrain was imposed on the maximum tube length: the heat exchanger doesn't exceed 2.5 m in length. In Table 2, also the values of each variable corresponding to the optimal solution of the problem are collected.

Table 1. Optimization model: constants

Constants	$T_{h,i}$ [°C]	$T_{h,o}$ [°C]	$T_{c,i}$ [°C]	$T_{c,o}$ [°C]	p_h [Pa]	p_c [Pa]	m_h [kg/h]	m_c [kg/h]	q [kW]
Value:	800	520	500	750	$1\ 10^5$	$4.5\ 10^5$	2220	2955	225

Table 2. Range of variability for each one of the identified parameters (variables) and optimal values obtained for these.

Variables	v_t [m/s]	Re_t 10^{-3}	N_p	$k_{L,tp}$	$k_{L,bc}$	k_{layout} *
Range of variability:	15÷25	10÷15	1÷2	1.3÷1.8	0.75÷1.0	1÷3
Identified values:	19	10.14	2	1.4	1.0	1

* k_{layout}, geometrical parameter for tube arrangement. Equal to 1 for 30° layout (i.e. triangular mesh), 2 for 90° layout (i.e. square mesh) and 3 for 45° layout (i.e. 45° square rotated mesh)

By keeping constant the fluids temperatures and the mass flow rates both at the cold and hot side of the heat exchanger (i.e. at constant thermal load of 225 kWth), the maximization of the global heat transfer coefficient U, as expressed by Eq. (2), and the minimization of the heat exchanger purchase cost C_t, as expressed by Eq. (6), were imposed. Because of the purchase cost is directly proportional to the global heat transfer area, A_o, only one objective function was considered for the minimization process. Main results of the optimizations are showed in the Figure 2-(b) and (c) respectively for the total heat transfer coefficient and the total heat transfer area both as function of the purchase cost of the equipment. In the same figures the Pareto frontiers were highlighted (red dots). As above explained these contain only the no-dominated solutions of the problem among which the optimum can be found. In order to identify this latter, furthers constrains were imposed on the Pareto solutions: the minimization of the pressure drops both at tube and at shell sides. These latter are operational constrains that directly influence the performances of the turbine. According to this the best solution of the problem among that lying on the Pareto frontier, is that which minimize the operative pressure losses. Main geometrical results for the optimum heat exchanger configuration are collected in Table 3. In more details, the operational optimum can be found by analysing data shown in Figure 3, where the global heat transfer coefficient, the global transfer area, pressure drops (both at shell and tube sides) and the heat exchanger purchase cost as function of the flow velocity at tube side are collected. The showed diagrams were obtained by considering only solutions that lie on the Pareto frontier (i.e. by considering among data only the solutions that optimize the mathematical problem as reported in Table 2 – identified values). As shown, the identified solution, Figure 2 – (b), minimize both the purchase cost and pressure drop at shell side, but doesn't maximize the global heat transfer coefficient, Figure 2 – (a). As expected as velocity at tube side increases, the global heat transfer coefficient increases too as consequence of the improved heat transfer coefficients both at tube and shell sides (higher Reynold's numbers). This in last instance means that, at given thermal load, the global transfer area decreases as velocity increases. Because of frictional losses are directly proportional to the fluid velocity ($\propto v_t^2$) also pressure drop increases.

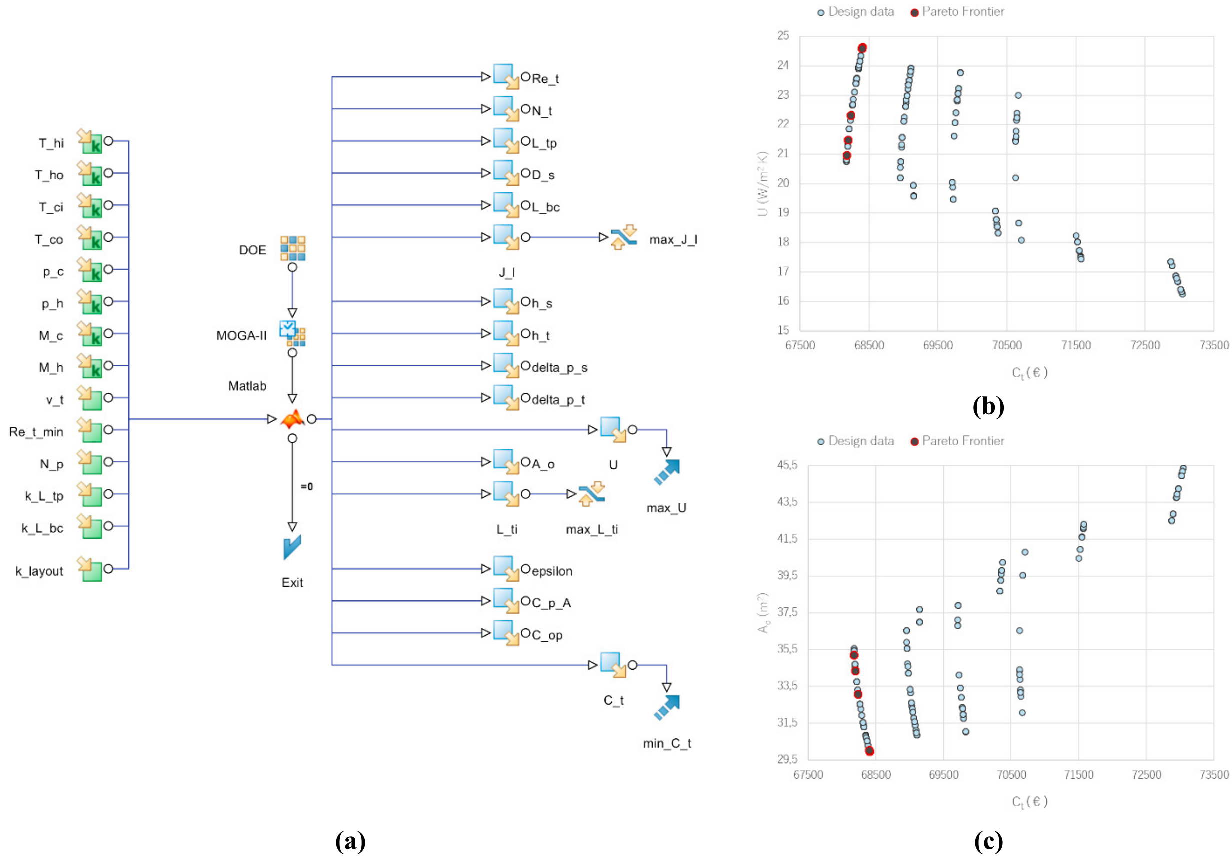

Figure 2. ModeFrontier® heat exchanger model (a), and main optimization results: global heat transfer coefficient vs. heat exchanger purchase cost (b); global heat transfer area vs. heat exchanger purchase cost (c).

Table 3. Main geometrical results for the optimum heat exchanger configuration.

Output	A_o [m^2]	$L_{t,i}$ [m]	N_t	D_s [m]	L_{bc} [m]	L_{tp} [m]	U [W/m^{2}K]	ΔP_s [Pa]	ΔP_t [Pa]	C_t [k€]
Optimal value:	35.56	2.46	76	0.75	0.82	0.073	20.75	338.22	284.57	68.17

In summary, as reported in the above tables, the optimized geometrical configuration, results in a two tube passes shell and tube heat exchanger with a total heat transfer area of 35 m^2, 76 tubes, internal shell diameter of 0.75 m and total tube length of about 2.50 m. The pressure drops both at shell and tube sides is below 0.5 kPa. By considering Alloy 800HT as fabrication material a total investment cost (actualized to 2018) of about 70 k€ (0.3 k€/kW$_{th}$) was obtained.

4. Conclusions

In this paper a new configuration where syngas produced by a downdraft gasifier is directly burned in a post combustion section to drive an externally fired micro-turbine was introduced. To achieve higher plant electrical efficiency, high temperatures are required at the turbine inlet section (above 700°C). All this makes the heat exchanger the critical component of this solution. Thought different type of heat exchangers can be theoretically applied such as plate heat exchangers, very high temperatures of flue gases (above 800°C) and fouling related issues drive the choice towards a more robust design: shell and tube configuration.

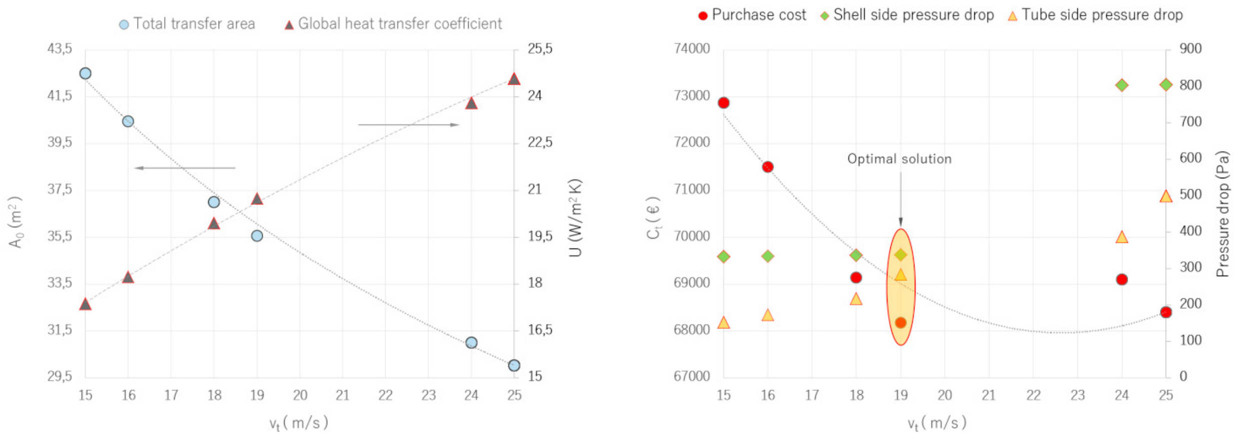

(a) **(b)**

Figure 3. Total heat transfer area, global heat transfer coefficient (a), heat exchanger purchase cost and pressure drops (b) as function of the fluid velocity at tubeside. The reported diagrams were obtained by considering as constants all parameters (variables) with the exception of fluid velocity as reported in Table 2 (i.e. the optimal values - identified values - for the variables were used).

A mathematical model of the heat exchanger according to TEMA standard and by using the Bell-Delawere detailed design method, was built by using Matlab®. In order to maximize the global heat transfer coefficient and minimize the total purchase cost, a geometrical optimization was performed by using a genetic multi-objective algorithm implemented in modeFrontier®. The calculations were performed by keeping constant the fluids temperatures and the mass flow rates both at the cold and hot side of the heat exchanger (i.e. at constant thermal load of 225 kW_{th}) and by considering eight main equipment operational constants and six geometrical and flow variables. Up to 10000 evaluations of the two objective functions were obtained defining among these the Pareto frontiers on which lying the optimal solution. In last instance, a two tube passes shell and tube heat exchanger with a total heat transfer area of 35 m^2, 76 tubes, internal shell diameter of 0.75 m and total tube length of about 2.50 m was found. By considering Alloy 800HT as fabrication material a total investment cost (actualized to 2018) of about 70 k€ (0.3 k€/kW_{th}) was obtained.

References

[1] Tapas Kumar Patra, Nimisha K.R., and Pratik N. Sheth, "A comprehensive dynamic model for downdraft gasifier using heat and mass transport coupled with reaction kinetics," *Energy*, no. 116, pp. 1230 - 1242, 2016 - https://doi.org/10.1016/j.energy.2016.10.036.

[2] Prakashbhai R. Bhoi, Raymond L. Huhnke, Sunil Thapa Ajay Kumar, and Natarianto Indrawan, "Scale-up of a downdraft gasifier system for commercial scale mobile power generation," *Renewable Energy*, no. 118, pp. 25 - 33, 2018 - https://doi.org/10.1016/j.renene.2017.11.002.

[3] Felipe O. Centeno González, Khamid Mahkamov, Electo E. Silva Lora, Rubenildo V. Andrade, and René Lesme Jaen, "Prediction by mathematical modeling of the behavior of an internal combustion engine to be fed with gas from biomass, in comparison to the same engine fueled with gasoline or methane," *Renewable Energy*, vol. 60, pp. 427-432, 2013 - https://doi.org/10.1016/j.renene.2013.05.037.

[4] A.A.P. Susastriawana, Harwin Saptoadi, and Purnomo, "Small-scale downdraft gasifiers for biomass gasification: A review," *Renewable and Sustainable Energy Reviews*, no. 76, pp. 989 - 1003, 2017 - http://dx.doi.org/10.1016/j.rser.2017.03.112.

[5] P. C. Roy, A. Datta, and N. Chakraborty, "An assessment of different biomass feedstocks in a downdraft gasifier for engine application," *Fuel*, vol. 106, pp. 864-868, 2013 - https://doi.org/10.1016/j.fuel.2012.12.053.

[6] Luiz Inácio Chaves, Marcelo Joséda Silva, Samuel Nelson Melegaride Souza, and et al., "Small-scale power generation analysis: Downdraft gasifier coupled to engine generator set," *Renewable and Sustainable Energy Reviews*, vol. 58, pp. 491-498, 2016 - https://doi.org/10.1016/j.rser.2015.12.033.

[7] "TEMA, Standards of Tubular Exchanger Manufacturers Association," Association, Tubular Exchanger Manufacturers, Tarrytown, NY, 2007.

[8] R. Mukherjee, "Effectively design shell and tube heat exchangers," *hem. Eng. Prog., Am. Inst. Chem.*, vol. 94, no. 2, pp. 21–37, 1998.

[9] Kuppan Thulukkanam, *Heat exchanger design handbook*.: CRC Press, 2013.

[10] Silvia Poles, "MOGA-II. An improved Multi-Objective Genetic Algorithm," ESTECO, 2003.